Assessment of concentrated solar power generation potential in China based on Geographic Information System (GIS)

Fuying Chen[1,2], Qing Yang[1,2,3,4*], Niting Zheng[2], Yuxuan Wang[5], Junling Huang[6], Lu Xing[7], Jianlan Li[2], Shuanglei Feng[1], Guoqian Chen[8], Jan Kleissl[9]

[1] *State Key Laboratory of Operation and Control of Renewable Energy & Storage Systems, China Electric Power Research Institute, Beijing 100192, P.R. China*

[2] *State Key Laboratory of Coal Combustion, Huazhong University of Science and Technology, 1037 Luoyu Road, Wuhan, Hubei 430074, P.R. China*

[3] *China-EU Institute for Clean and Renewable Energy, Huazhong University of Science and Technology, Wuhan 430074, P.R. China*

[4] *John A. Paulson School of Engineering and Applied Sciences, Harvard University, Cambridge, MA 02138, USA*

[5] *School of electronic & electrical engineering, University of Leeds, Leeds, LS2 9JT, UK*

[6] *International Clean Energy Research Office, China Three Gorges Corporation, Beijing, P.R. China*

[7] *Engineering and Environment Faculty, Northumbria University, Newcastle upon Tyne, NE1 8ST, UK*

[8] *College of Engineering, Peking University, Beijing 10084, P.R. China*

[9] *Department of Mechanical & Aerospace Engineering, University of California, San Diego, La Jolla, CA, 92093, USA*

* Corresponding authors: State Key Laboratory of Operation and Control of Renewable Energy & Storage Systems, China Electric Power Research Institute, Beijing 100192, P.R. China.

E-mail address: qyang@hust.edu.cn (Q. Yang).

Abstract

Concentrating solar power (CSP) technology can not only match peak demand in power systems but also play an important role in the carbon neutrality pathway worldwide. Actions in China is decisive. Few previous studies have estimated CSP technology's power generation and CO_2 emission reduction potentials in China. To address this knowledge gap, the geographical, technical, and CO_2 emission reduction potential of CSP in China was evaluated by province based on a high resolution geographical information system with up-to-date data. A comprehensive framework including geographic and technical constrains was proposed. Exclusion criteria including solar radiation, slope, land-use type, natural reserve, and water resources were adopted to determine the suitability of CSP plant construction. Then, based on the power conversion efficiency difference from various CSP technologies, the technical potential was calculated on suitable land. The results show that approximately 1.02×10^6 km^2 of land is available to support CSP development in China. Based on the available solar resource on the suitable land, the geographical potential is 2.13×10^{15} kWh. The potential installed capacity is 2.45×10^7–5.40×10^7 MW, considering four CSP technologies. The corresponding annual energy generation potential is 6.46×10^{13}–1.85×10^{14} kWh. Considering the scenario of using the potential of CSP to replace the current power supply to the maximum extent, CO_2 emission would have been reduced by 5.19×10^8, 5.61×10^8, and 6.24×10^8 t in 2017, 2018, and 2019, respectively. At the provincial level, more than 99% of China's technical potential is concentrated in five western provinces, including Xinjiang, Inner Mongolia, Qinghai, Gansu, and Tibet. These results provide policy guidance and serve as a reference for the future development of CSP and site selection for CSP plant construction both in China and worldwide.

Keywords: Concentrated solar power, Geographic information system, Resource assessment

Nomenclature

Item	Definition
CSP	Concentrating solar power
PV	Photovoltaic
PTC	Parabolic trough collector
LFC	Linear Fresnel collector
sCO_2	Supercritical carbon dioxide
CRS	Central receiver system
PDS	Parabolic dish system
DEM	Digital elevation model
DNI	Direct normal irradiance
GIS	Geographical information system
NEA	National Energy Administration
PG	Power generation
LA	Land area
EFF	Efficiency
LUF	Land-use factor
PC	Potential capacity
LCF	Land conversion factor
UHV	Ultra-high voltage
ER	Emission reduction
EF	Emission factor
PD	Power demand
LCOE	Levelized cost of electricity

1. Introduction

At present, more than 130 countries and regions have proposed "zero carbon" or "carbon neutral" climate goals [1]. Meanwhile, speeding up the clean and low-carbon energy technologies development to overcome global challenges related to climate change and sustainable development has become the international community's universal consensus and concerted action [2]. The energy transition strategy of the European Union and its Member States has been basically based on the integration of renewable energy technologies in the national grid [3]. However, one of the most significant challenges of this strategy is that the high proportion of renewable energy technologies has brought considerable obstacles to grid management and strengthened the demand for peak shaving units [3].

Concentrated solar power (CSP) is a promising solar thermal power technology that can participate in power systems' peak shaving and frequency support [4,5]. Compared with solar photovoltaics (PV), wind power, and other power technologies with strong output fluctuation, CSP can integrate a large-capacity heat storage system to ensure smooth power generation output and improve the flexibility of power delivery to the grid [6,7]. CSP plants also have a ramping ability and generation range equivalent to gas-fired units, superior to ordinary thermal power units [8]. The life cycle greenhouse gas emissions of CSP are lower than conventional sources [9]. Therefore, a CSP plant integrated with thermal energy storage can play an important role in providing ancillary services to power grids with high renewable penetration, especially in multi-energy systems [10].

China's action is decisive for international goals. To deal with climate change, China has put forward a new goal of "striving to achieve carbon peak by 2030 and carbon neutrality by 2060" [11]. The trend of various typical electrification indicators continues to improve, which shows that China's electrification is advancing rapidly [12]. Achieving carbon neutrality in the power sector mainly relies on promoting more renewable energy to be used on a large scale through conversion to electricity [13]. However, the problem of grid-connected consumption has begun to emerge, and the

problem of abandoning wind and solar has become more prominent. Therefore, as the proportion of fluctuating renewable energy sources in the power grid continues to increase in the future, CSP with large-capacity heat storage will be an attractive energy source as it can regulate the power system peak output.

Since an electric system with high renewable penetration in China could be decisive for averting the global climate crisis, it is imperative to determine the power generation potential of CSP and its geographic distributions in the country. The relevant research in China is still insufficient. The potential for solar energy generation can be classified as geographical and technical. The geographical potential is the annual total solar radiation in a suitable regional area, taking into account geographic constraints [14]. Northwest China is rich in solar energy resources, and the annual average solar radiation can reach 1750 kWh/m^2 [15]. Solar radiation received on the surface in China was estimated to be up to 5.28×10^{16} MJ [16].

However, not all solar resources can be used for power generation, depending on the specific land-use type and other geographic constraints, e.g., nearby available water resources and slope. In terms of land use, most studies eliminated protected areas first, including national parks, safari areas, historical and touristic monuments, and natural reserves [17,18,19,20]. Uyan et al. established a 0.5-km buffer zone for a natural reserve [21]. Similarly, most studies excluded water bodies such as rivers, lakes, and wetlands [22,23]. In addition to a protected area and water body, Hermann et al. excluded agricultural zones and forests [24]. Barren and low-productivity areas were suggested to be the priority locations for solar energy plants [25]. Sharma et al. selected five types of wasteland suitable for CSP station construction [26]. Different technology types of CSP stations have different slope requirements, wherein parabolic trough collector (PTC) and linear Fresnel collector (LFC) techniques are particularly limited by the slope [27]. Djebbar et al. excluded areas with slopes exceeding 1%–4% [22]. Water resource constraints should also be considered. While other renewable energy technologies such as solar PV or wind power use relatively little water, CSP with wet cooling – like most thermal power technologies - requires a considerable amount of water, mainly for cooling [28]. Supercritical carbon dioxide (sCO_2) Brayton cycle

technology can significantly reduce water consumption, but it has not yet reached commercial application in China [29]. At present, the CSP station mainly adopts the steam turbine for power generation, which has high requirements for water resources [29]. Tlhallerwa et al. adopted air cooling technology to provide greater siting flexibility because air cooling reduces the water demand by 90% compared with water cooling [30]. Giamalaki et al. considered that the use of water to cool the CSP system would cause severe environmental pollution owing to the thermal pollution of the water body; therefore, a site located at a long distance from water resources was determined to be suitable [25]. However, since dry cooling increases costs and reduces efficiency [30], the construction of CSP stations using wet cooling technology is preferred in the vicinity of water resources [19,31]. Other factors, including the distance to roads and power grids were taken into account [32]. In addition, the distance to settlements was also considered [33,34]. Boukelia et al. took proximity to the transmission-line corridor and natural gas pipeline as constraints [35].

The technical potential of solar energy generation in the selected area can be defined as the geographical potential of the area, which can be converted into electrical energy under the conditions of existing solar power technology [14]. CSP technologies can be classified into four types: parabolic trough collector (PTC), linear Fresnel collector (LFC), central receiver system (CRS), and parabolic dish system (PDS). The schematic view of the applied technologies is shown in Fig. 1. Solar collectors receive maximum solar radiation at the optimum slope and surface azimuth [36,37]. Optimizing the heliostat layout of the CSP plant can achieve maximum heliostat field efficiency [38]. Therefore, it is assumed that the mirror fields are equipped with tracking devices and arranged according to the optimum mirror slope and ground azimuth. The power generation potential of the PTC was often calculated as technical potential because it represents the largest proportion and most mature CSP technology currently in the market [30,31,34]. Few studies have considered the four different CSP technologies and calculated their annual power generation based on the average solar-to-electric conversion efficiency [39,40].

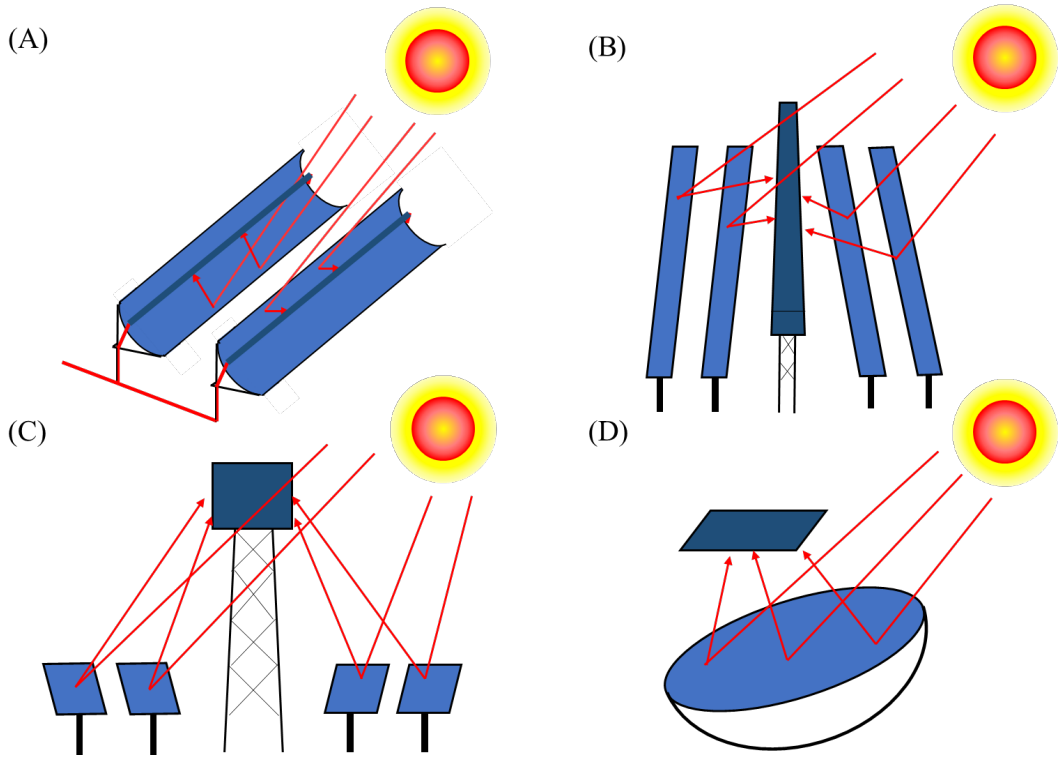

Fig. 1. The schematic view of four CSP technologies: (A) Parabolic trough collector (PTC), (B) linear Fresnel collector (LFC), (C) central receiver system (CRS), and (D) parabolic dish system (PDS).

For geographical potential, a few studies have proposed the framework for screening suitable areas for the CSP plants construction and evaluated the CSP potential in specific areas in China. Early in 2007, Wang et al. proposed a decision support system framework for site selection of CSP plants based on geographic constrains [41]. Then, according to the annual mean solar radiation of 97 stations, the radiation distribution with a resolution of 1 km in China was obtained by spatial interpolation [41]. Zhao et al. established a screening index using the analytic hierarchy process to calculate the weights of related factors, then applied the screening method to select suitable places for planning CSP plants in Inner Mongolia [42,43]. Wu et al. proposed a more complete and practical multi-criteria decision-making framework for PTC solar power plant location selection [44]. Then, case studies were conducted in five cities in Western China to find the most suitable location for CSP stations [44]. However, the above studies did not apply their land screen method to the nation. For nationwide CSP

technical potentials, He et al. adopted 10-year (from 2001 to 2010) hourly solar radiation data from 200 representative sites in China to screen the areas suitable for developing CSP plants considering geographic constraints [45]. Moreover, the annual power generation and the installed capacity of potential CSP plants were calculated by province based on an average land use conversion factor [45]. However, due to technical data unavailability, the difference in the results of different CSP technologies was ignored. Water resources availability, usually considered an important factor, was also ignored in He et al.'s study [45]. On the other hand, the data used in He et al.'s study is the most accurate data at that time, such as solar irradiance data for 200 chosen locations, land cover dataset, and the digital elevation model (DEM) dataset with 1 km ×1 km resolution, however, the data quality is improving with time, and higher data resolution will allow more accurate estimation. Therefore, compared with the previous studies in China, there are improvements and innovations in the methodological framework, data accuracy, and result resolution.

To narrow the knowledge gap, it is necessary to assess the geographical, technical, and CO_2 emission reduction potential of CSP in China based on a high resolution geographical information system with up-to-date data and more concerns on water resource availability. The novelties of this study compared with previous studies in China are as follows: first, a comprehensive framework was proposed to evaluate geographic and technical CSP potentials and associated GHG emission reduction potentials for the first time. Geographic constrains included five factors: solar radiation, slope, land-use type, natural reserve, and water resources. Among them, in the previous studies in China, water resources were often ignored, but it was an important factor in the screening framework and should be considered. At the same time, the power conversion efficiency difference from various CSP technologies was considered in technical constrains. Second, accurate and reliable data were adopted, such as direct normal irradiance (DNI) data, from 2008 to 2017, with a spatial resolution of 9 km and temporal resolution of 1 h. This is the first time that the non-public data has been used to assess China's CSP potential. Besides, land cover data came from an essential achievement of China's 863 Program, with a spatial resolution of 30 m. Third, to allow

evaluating the geographical and technical potential of CSP plants in the context of grid needs and constrains, the results are presented at a more granular level by province. Therefore, this research aimed to accurately assess the geographical and technical potential of CSP stations, and provide a scientific basis and data base for CSP development plans in various provinces in China.

2. Material and methods

2.1 Geographical information system (GIS) tool and criteria overview

The framework for assessing the geographical, technical, and CO_2 emission reduction potential of CSP in China is illustrated in Fig. 2. The land conversion factor is the ratio of the power plant's installed capacity to the ground area. Land use efficiency includes solar-to-electric conversion efficiency and land use factor, which is the ratio of the reflector area to the total area of the power station [30]. This study established screening principles to select suitable locations for CSP plant construction. ArcGIS version 10.4.1 has rich functions and comprehensive processing capacity, applied to process all collected data [32]. Based on previous research, five criteria (i.e., solar radiation, protected areas, land use, slope percentage, and distance from water resources) were considered. However, there was no agreement in the literature on standard threshold values of site selection for CSP construction in China. Therefore, the threshold values in this study were based on the first CSP demonstration projects in China and the previous studies. Table 1 provides information regarding the first CSP demonstration projects [44,46,47]. The missing area for some plants is due to the slow development of CSP in China, with more than half of the first batch of demonstration projects still under construction or suspended. System conversion efficiency was estimated by the company when establishing a project.

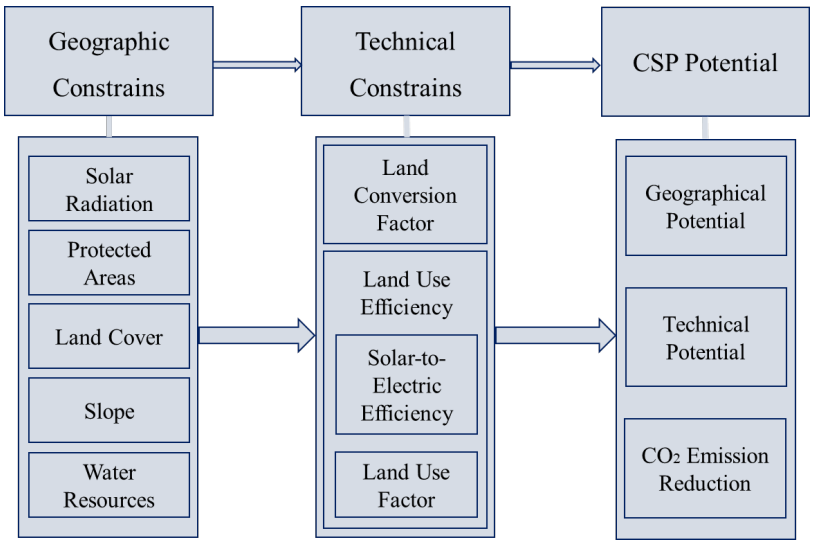

Fig. 2. Research framework of this study.

2.2 DNI

Unlike PV technology, which can use both direct and diffuse solar irradiance, CSP technology converts only DNI to electricity [48]. DNI is the most basic and vital factor in the location selection of CSP stations because it directly affects the efficiency and economics of the plant [49]. Ziuku et al. believed that commercial development of the CSP project required the site with DNI of at least 2000 kWh/m^2 [17]. Djebbar et al. set minimum DNI limits at 1500 kWh/m^2 [22]. A study on estimating the CSP potential of Africa excluded areas with DNI < 1800 kWh/m^2 [24]. According to the "Notice on Organizing the Construction of Solar Thermal Power Demonstration Projects" issued by the National Energy Administration (NEA), DNI at the site should be more than 1600 kWh/m^2 [50]. Therefore, in this study, the threshold of 1600 kWh/m^2 was set to eliminate inappropriate areas. DNI data were obtained from the Renewable Energy Department of China Electric Power Research Institute, which generated meteorological data for China for 2008–2017 with a 9-km spatial resolution and a 1-h temporal resolution numerical weather prediction model.

Table 1. Relevant data of the first batch of demonstration projects of concentrating solar power (CSP) plants in China [44,46,47]. DNI - direct normal irradiance, CRS – central receiver system, PTC – parabolic trough collector, LFC – linear Fresnel collector.

Technology	Project name	Long.	Lat.	DNI ($kWh/m^2/yr$)	Area (km^2)	Thermal energy storage capacity (h)	System conversion efficiency (%)
CRS	Qinghai Supcon Delingha 50 MW molten salt	97.36°	37.37°	1976	2.40	6	18
	Dunhuang 100 MW molten salt	94.48°	40.14°	2000	7.84	11	16
	Qinghai Gonghe 50 MW molten salt	100.9°	36.40°	1900	/	6	16
	Hami 50 MW molten salt	93.45°	42.89°	1920	/	8	16
	Delingha 135 MW direct steam generation	97.36°	37.37°	1900	/	4	15
	Gansu Jinta 100 MW molten salt	98.74°	40.01°	1900	6.00	8	16
	Shangyi 50 MW direct steam generation	113.9°	41.07°	1600	/	4	17
	Yumen 50 MW molten salt	97.93°	39.81°	1800	2.47	6	19
	Yumen 100 MW molten salt	97.05°	40.29°	1800	6.80	10	17
PTC	Yumen East Town 50 MW thermal oil (Royal tech CSP Co., Ltd..)	97.92°	39.81°	1800	2.48	7	25
	Yumen East Town 50 MW thermal oil (Rayspower Energy Group Co., Ltd.)	97.05°	40.29°	1800	2.90	7	25

	Gansu Akesai 50 MW molten salt	94.37°	39.62°	2056.5	/	15	21
	Urat Middle Banner 100 MW thermal oil	108.51°	41.59°	2025	4.67	4	27
	Delingha 50 MW thermal oil	97.36°	41.59°	1976	2.60	9	14
	Gansu Gulang 100 MW thermal oil	102.90°	37.47°	1913	/	7	22
	Zhangjiakou 64 MW molten salt	114.94°	41.42°	1700	2.87	16	22
LFC	Dunhuang 50 MW molten salt	94.48°	40.14°	2000	3.19	13	17
	Urat Middle Banner 50 MW thermal oil	108.52°	41.59°	2025	/	6	19
	Zhangbei 50 MW direct steam generation	114.72°	41.07°	1750	/	14	11
	Zhangjiakou 50 MW direct steam generation	114.72°	41.07°	1750	/	14	12

2.3 Protected areas

The establishment of protected areas is a fundamental measure of biodiversity conservation, which plays an essential role in climate change mitigation and adaptation. According to the design standard for CRS solar power stations issued in 2018, site selection should align with the national medium and long-term development plan, and natural reserves should be avoided [51]. Natural reserve data were obtained from the World Database on Protected Areas, and ecological functional reserve data were adopted from the Chinese Academy of Sciences Resource and Environment Science and Data Center; both were excluded from consideration for the construction of CSP plants.

2.4 Land cover

Land cover information was provided by the GlobeLand30 dataset of the National Catalogue Service for Geographic Information. The dataset contained 10 main land-cover types, including cultivated land, forest, grassland, shrubland, wetland, water bodies, tundra, artificial surfaces, bareland, and permanent snow & ice. Ideally, CSP station construction should occur on unused and low-productivity agriculture or pasture areas and areas usually covered by grassland or shrubland to minimize the impact on land use [52]. However, for power stations that have been built in China, the lands used in the projects include desert and other state-owned unused lands [53]. Therefore, bareland was selected as a land type that can construct CSP stations.

2.5 Slope percentage

Flat and wide lands are optimal for CSP station construction because the construction costs go up for land levelling [25]. Giamalaki et al. considered the slope less than 4.0° was particularly suitable [25]. Ziuku et al. set the upper boundary of suitable slopes to 1.7° [17]. In the International Renewable Energy Agency studies, 2.1° was adopted as the upper limit [24,54]. Djebbar et al. considered a constraint of 0.6°–2.3° [22]. He et al. set 0.6° and 1.7° as the lower and upper limits, respectively [45]. Therefore, an intermediate value of 3° was adopted to be the upper limit in this study. The influence of the slope change on the results was discussed in the sensitivity analysis part. DEM data with a 500 m resolution were obtained from the Chinese Academy of

Sciences Resource and Environment Science and Data Center. The Arctoolbox in ArcGIS was applied to derive slope from the DEM data.

2.6 Distance from water resources

Because CSP systems still use a steam turbine to generate electricity from the solar heat, the demand for water consumption of CSP stations is similar to that of thermal power generation [55]. In addition, water resources are needed to clean the mirror to ensure the high reflection efficiency of the mirror field. Some water sources can be recycled; however, non-recyclable water sources need to be supplemented by local resources. CSP plants usually have two cooling methods: water and air cooling. The total amount of water required for air cooling is approximately 12% of that required for water cooling [56]. If air cooling technology is adopted, water consumption can be significantly reduced; however, this may be accompanied by a substantial increase in the investment cost (by approximately 7%–9%) and a reduction in power generation (by approximately 5%) [57]. Consequently, the CSP station should be near a water body. According to a document issued by the NEA, air cooling units should be adopted in principle for coal-fired power station projects in water-scarce regions in northern China. Therefore, in the northern water-deficient provinces (including Beijing, Tianjin, Hebei, Gansu, Inner Mongolia, Shanxi, Shaanxi, Henan, Jiangsu, Shandong, Anhui, Heilongjiang, Jilin, Liaoning, and Ningxia), CSP stations adopt air cooling technology, whereas water cooling is adopted in the remaining provinces. Therefore, the proximity to water resources was required to be less than 50 km based on previous literature and China's land area [17,18,19]. The distribution of water resources was provided by the National Catalogue Service for Geographic Information.

2.7 CSP generation potential

Through the five screening principles mentioned above and data processing operations in ArcGIS, the potential areas were screened out, and the area suitable for CSP generation was obtained for each province. Then, the annual generation capacity of the CSP station in different provinces was calculated using Eq 1, developed by Hermann et al [24].

$$\mathrm{PG} = \mathrm{LA} \times \mathrm{DNI} \times \mathrm{EFF} \times \mathrm{LUF}, \qquad (1)$$

where PG is the annual power generation (kWh); LA is suitable land area per the screening criteria (m^2); DNI is the annual average DNI per unit area (kWh/m^2); EFF is the solar-to-electricity conversion efficiency of the power station; and LUF is the land-use factor, which is the ratio of the reflector area to the total area of the power station. Since air cooling is required in northern China due to water scarcity, it will reduce the efficiency of CSP plants, resulting in a 5% reduction in the power generation in that area.

The potential installed capacity of the CSP plants was assessed using Eq 2, adopted by He et al. [45].

$$PC = LA \times LCF, \qquad (2)$$

where PC is the potential capacity (MW); and LCF is the land conversion factor, which is the ratio of the power plant's installed capacity to the ground area (MW/km^2). Land conversion factors vary owing to differences in technology [45].

The four CSP technologies differ in their power generation properties. There are differences in the land-use factor, land conversion factor, and solar-to-electric conversion efficiency due to changes in local conditions, array configuration, tracking technology, and thermal storage methods, as listed in Table 2 [34,49,58,59,60,61]. The upper and lower limits of solar-to-electric conversion efficiency were used to calculate the interval value of power generation.

Table 2. Parameters of different concentrating solar power (CSP) technologies. PTC - parabolic trough collector, LFC - linear Fresnel collector, CRS - central receiver system, PDS - parabolic dish system [34,49,58,59,60,61].

Technology	Land-use factor (%)	Land conversion factor (MW/km^2)	Annual solar-to-electric conversion efficiency (for water cooling, %)
PTC	28	26	11–21
LFC	49	53	8–18
CRS	23	24	15–35
PDS	22	25	25–30

2.8 CO_2 emission reduction potential of CSP plants

In 2016, the NEA officially approved the first batch of demonstration projects of CSP plants in China. The CO_2 emission reduction potential in 2017–2019 was calculated based on the CRS technology, wherein the land-use factor was assumed to be 23%, and the solar-to-electric conversion efficiency was assumed to be 25%. China made a voluntary carbon reduction commitment at the 2015 Paris Climate Conference, whereby CO_2 emissions would peak by 2030. CSP stations reduce CO_2 emissions by replacing traditional power stations. In this study, it was assumed that CSP plants can replace the current power generation mode to the maximum extent, based on which two scenarios were established. Scenario one assumed that the province-to-province absorption capacity of ultra-high voltage (UHV) transmission lines in China was limited. If the local CSP generation potential cannot meet the power demand, the generation potential is the maximum power supply substitution value for these provinces. This means that CSP generation can reduce CO_2 emissions by replacing part of the electricity supply. The CO_2 emission reduction is calculated as following [62]:

$$\mathrm{ER} = (\mathrm{EF} - \mathrm{CSPEF}) \times \mathrm{PG}, \qquad (3)$$

where ER is the CO_2 emission reduction (kg CO_2); EF is the grid emission factor (kg CO_2/kWh); CSPEF is the life cycle CO_2 emission intensity of CSP plants (kg CO_2/kWh); and PG is the potential of solar thermal power generation (kWh).

If the power generation potential is greater than the power demand, then the excess generation is curtailed, and Equation (3) becomes [62]:

$$\mathrm{ER} = (\mathrm{EF} - \mathrm{CSPEF}) \times \mathrm{PD}, \qquad (4)$$

where PD is the local power demand in kWh, which can be obtained from the "China Statistical Yearbook" issued by the National Bureau of Statistics [63]. In Scenario 2, it was assumed that the UHV power grid could fully transmit excess generation across provinces to achieve a complete replacement of the existing power supply with CSP generation. Therefore, the CO_2 emission reduction in each province under Scenario 2 was calculated from Equation 3.

China’s power grid is divided into six regions (excluding Tibet, Hong Kong, Macau, and Taiwan, which are not discussed in this paper). The emission factors from

the power grids of each region in China vary according to the local power sources. The CO_2 emission factor of each region consists of the operating margin and build margin obtained from the Institute for Global Environmental Strategies [64]. Operating margin refers to the emission factor for marginal emissions related to the operation of a set of existing power plants whose current power generation will be influenced [62]. Build margin refers to the emission factor for marginal emissions related to the construction process of a set of potential power plants whose construction and future operation will be influenced [62]. Combined margin is the weighted average of operating margin and build margin [65]. In this study, the emission weight of the two parts was taken as 0.5 [65]. The 2015-2017 emission factors were assumed and are shown in Table 3.

Although CSP plants are generally considered to have little negative environmental impact, from a life-cycle perspective, CO_2 emissions are still generated during the construction and material production stages [9,27]. According to Li [66], the life-cycle carbon footprint of a central receiver system CSP plant is 0.035 kg/kWh. The summary of data sources is shown in Table 4.

Table 3. Grid emission factors of China in 2015–2017 (kg CO_2/kWh) [64].

Regional grid	Operating margin	Build margin	Combined margin
North China Grid	1.0032	0.4621	0.7327
Northeast China Grid	1.1181	0.4015	0.7598
East China Grid	0.8079	0.5449	0.6764
Central China Grid	0.9253	0.3227	0.6420
Northwest China Grid	0.9309	0.2920	0.6115
Southern China Grid	0.8667	0.3065	0.5866

Table 4. The summary of data sources. DNI - direct normal irradiance, DEM - Digital elevation model.

Data	Descriptions	Sources
DNI	Raster data, Time span: 2008-2017, Temporal resolution: 1 h, Spatial resolution: 9 km	Renewable Energy Department of China Electric Power Research Institute (Non-publicise)
Natural reserve	Vector data	World Database on Protected Areas (https://www.protectedplanet.net/country/CHN)
Ecological functional reserve	Vector data	Chinese Academy of Sciences Resource and Environment Science and Data Center (https://www.resdc.cn/data.aspx?DATAID=137)
Land cover	Raster data, Spatial resolution: 30 m	National Catalogue Service for Geographic Information (https://www.webmap.cn/commres.do?method=dataDownload)
DEM	Raster data, Spatial resolution: 250 m	Chinese Academy of Sciences Resource and Environment Science and Data Center (https://www.resdc.cn/data.aspx?DATAID=123)
Water resources	Vector data	National Catalogue Service for Geographic Information (https://www.webmap.cn/commres.do?method=dataDownload)
Local power demand	Time span: 2017-2019	China Statistical Yearbook (http://www.stats.gov.cn/tjsj/ndsj/2020/html/C0914.jpg)
Grid emission factor	Time span: 2015-2017	Institute for Global Environmental Strategies (https://www.iges.or.jp/en/pub/list-grid-emission-factor/en)

3. Results and discussion

3.1 Geographical potential

The collected DNI meteorological file data were imported into GIS for processing and overlayed onto the map of China to obtain Fig. 3. As shown in Fig. 3, the best solar energy resources in China are mainly concentrated in the western regions of Inner Mongolia, Tibet, Qinghai, Xinjiang, Gansu, Yunnan, and Sichuan. The annual mean DNI of these areas is between 1700 and 3100 kWh/m^2, which satisfies the standard for establishing CSP stations per Section 2.1.

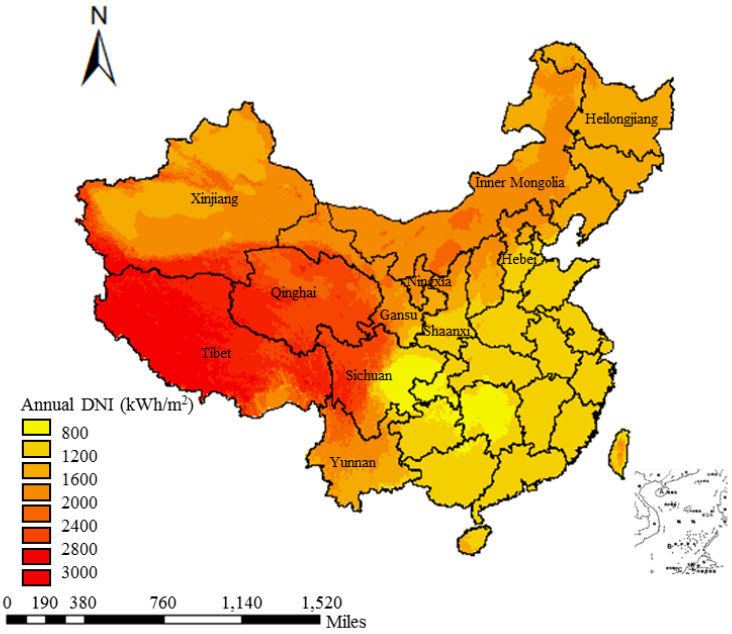

Fig. 3. Annual mean direct normal irradiance (DNI) of each province in China (kWh/m^2).

Then, based on the five exclusion criteria, the suitable areas for CSP plant construction were identified, as shown in Fig. 4. Fig. 4 also shows the locations of the first CSP demonstration projects in 2016, which are mostly consistent with the selected areas and are mainly concentrated in China's Xinjiang, Inner Mongolia, Qinghai, Gansu, and Tibet. Because of the similar geographical locations of some demonstration power stations, the actual locations of the 20 power stations are not separately identifiable in Fig. 4. Then, the annual mean DNI of each province was obtained through GIS operation based on the annual mean DNI original data at the resolution of 9 km. The

geographical CSP potential in the suitable areas is summarized in Table 5. The total geographical potential can reach 2.13×10^{15} kWh. The total area suitable for construction was 1.02×10^{6} km^2, accounting for approximately 11% of the national area. Xinjiang, Inner Mongolia, Qinghai, Gansu, and Tibet (i.e., the five northwestern provinces) occupy only 52.69% of the land area in China but represent 99.62% of the CSP potential area. Although the suitable land area of Tibet is smaller than that of Gansu, its geographical potential is higher than that of Gansu owing to the more abundant solar resources. The DNI distribution in the suitable area was also visualized (Fig. 5). Of note, a minimum DNI of 1600 kWh/m^2 was set in this study, which led to the exclusion of 14 provinces.

Table 5. Geographical potential of the suitable region of each province in China. DNI - direct normal irradiance. Provinces without suitable area are not shown.

Province	Annual mean DNI (kWh/m^2)	Suitable area (km^2)	Ratio of suitable area to total area (%)	Geographical potential (GWh)
Yunnan	2343.83	1.57×10^{0}	0.00	3.68×10^{3}
Heilongjiang	1613.25	2.14×10^{0}	0.00	3.45×10^{3}
Hebei	1926.07	1.87×10^{1}	0.01	3.60×10^{4}
Shaanxi	1926.55	1.03×10^{2}	0.05	1.98×10^{5}
Sichuan	2738.74	3.41×10^{2}	0.07	9.33×10^{5}
Ningxia	1742.12	3.38×10^{3}	6.88	5.89×10^{6}
Tibet	3247.14	9.65×10^{4}	8.12	3.13×10^{8}
Gansu	1936.64	1.13×10^{5}	29.58	2.19×10^{8}
Qinghai	2440.26	1.23×10^{5}	17.90	3.00×10^{8}
Inner Mongolia	1876.49	2.17×10^{5}	20.40	4.07×10^{8}
Xinjiang	1893.65	4.66×10^{5}	30.36	8.82×10^{8}

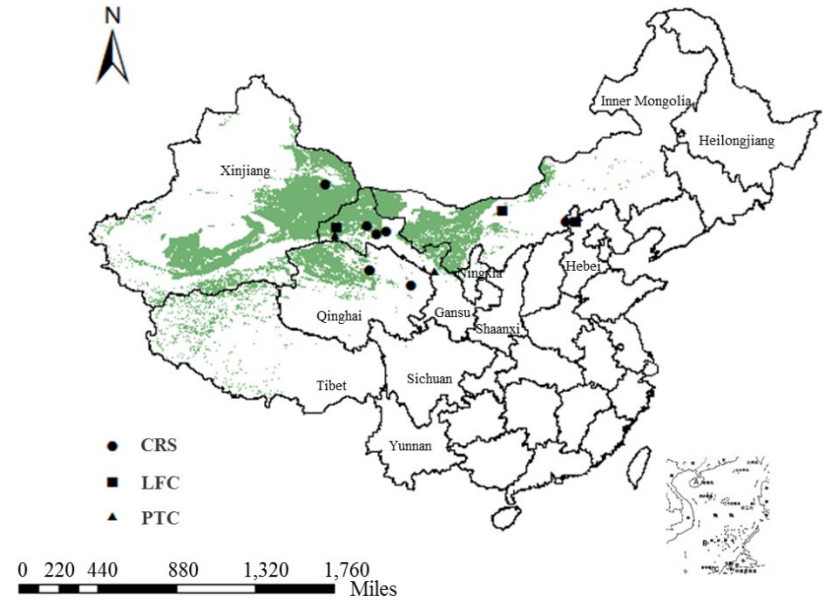

Fig. 4. Areas suitable for construction of concentrating solar power (CSP) stations in China in green. Markers show the locations of twenty demonstration projects sites in 2016: CRS - central receiver system, LFC - linear Fresnel collector, PTC - parabolic trough collector.

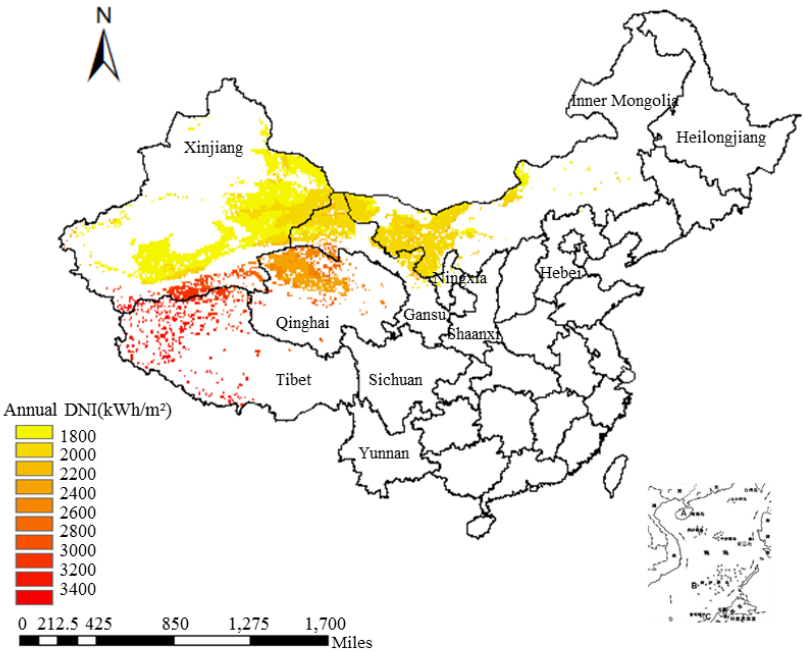

Fig. 5. Direct normal irradiance (DNI) distribution on suitable lands.

3.2 Technical potential

Based on the assessment of the geographical potential of the available area obtained using Equation 1 and the parameters in Table 3, the total annual power generation of CSP plants using four different technologies, i.e., PTC, LFC, CRS, and PDS, are 6.46×10^{13}–1.23×10^{14}, 8.22×10^{13}–1.85×10^{14}, 7.23×10^{13}–1.69×10^{14}, and 1.15×10^{14}–1.38×10^{14} kWh, respectively, which are 8.91–25.52 times the national electricity consumption in 2019. The corresponding installed capacities of CSP in China are approximately 2.65×10^{7}, 5.40×10^{7}, 2.45×10^{7}, and 2.55×10^{7} MW for PTC, LFC, CRS, and PDS, respectively, and 4,900–10,800 times the installed capacity target by the end of 2020 proposed in the 13th Five-Year Plan for Electric Power Development [67]. This reflects the abundance of solar energy resources in China and demonstrates the potential for the development of CSP technology. If CSP is developed according to its potential, it can generate a significant fraction of China's electricity consumption in the future.

Figure 6 shows the power generation and capacity potential of different CSP technologies in each province. The province with the largest power generation potential is Xinjiang, accounting for approximately 42.06% of the country's total power generation potential, and Tibet, Inner Mongolia, Qinghai, and Gansu account for 14.95%, 18.44%, 14.29%, and 9.94%, respectively. These five provinces account for 99.68% of the country's total power generation potential; however, they only accounted for 11.87% of the national electricity consumption in 2019. Similarly, the provinces with the highest installed capacities are Xinjiang, Inner Mongolia, Qinghai, Gansu, and Tibet. It can be concluded that future CSP development in China will focus on provinces in the northwest. The majority of the first batch of CSP demonstration stations is concentrated in Qinghai (4), Gansu (9), and Hebei (4), whereas only three stations are located in Xinjiang and Inner Mongolia, which are the provinces with the richest solar resources. The development of CSP technologies in Xinjiang and Inner Mongolia is difficult. The remoteness of these two provinces, the local lack of skilled labor and raw materials for establishing plants, and the need to import materials and supplies by train result in higher construction costs. However, after solving these problems, the rich

geographical potential in Xinjiang and Inner Mongolia has a great potential for power generation.

From the perspective of the technology type, LFC has a higher land conversion factor; therefore, its power generation potential is higher than that of the other three technologies (PTC, CRS, and PDS). Higher solar-to-electric conversion efficiency also improves the annual power generation of the power station. Therefore, while developing the CSP potential area, improving technology to reduce the cost and improve the efficiency of CSP can yield further gains in potential. In addition, thermal energy storage is an indispensable part of CSP installations [68], and all existing plants in China have storage capacities [69]. Thus, CSP technology with large-capacity thermal energy storage will enable peak load regulation of the power system. With increasingly mature thermal energy storage technology, annual power generation will also be further increased.

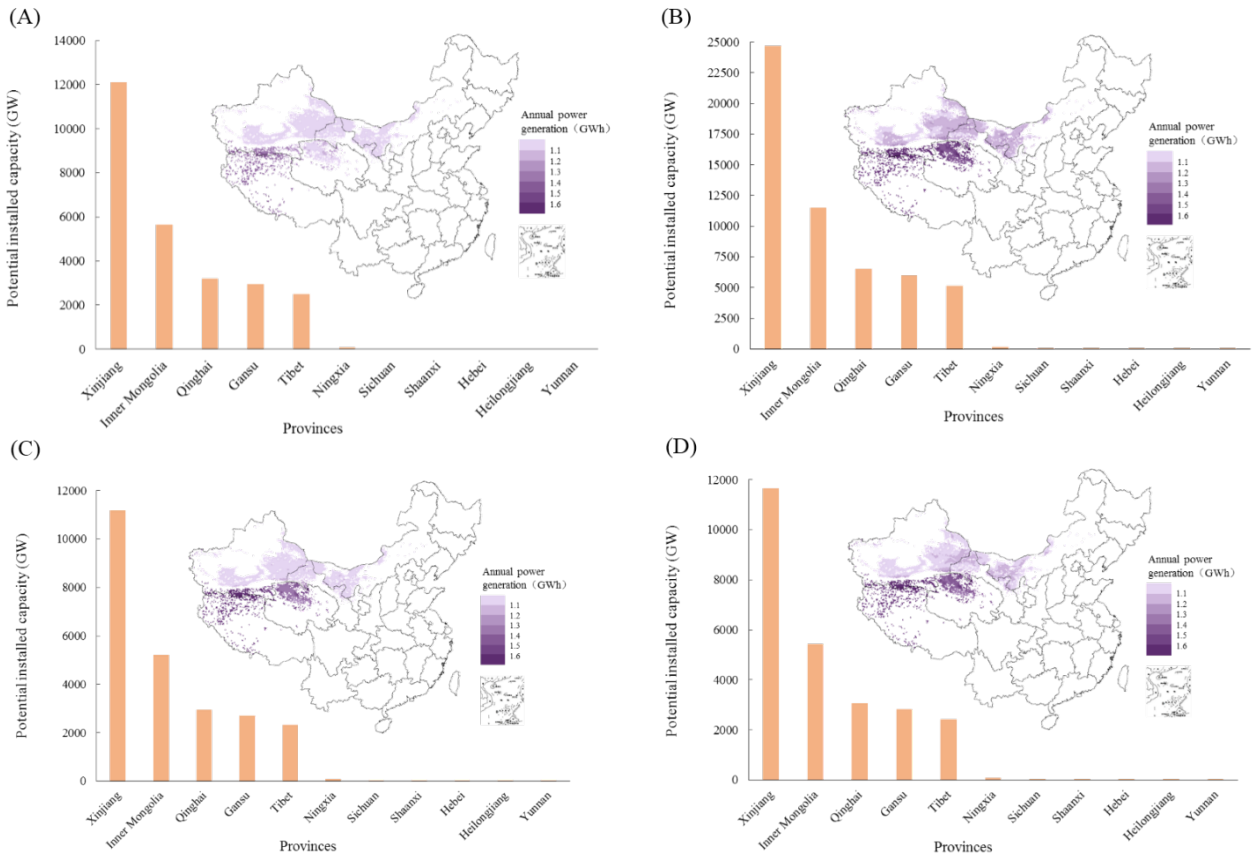

Fig. 6. Annual power generation and potential installed capacity of concentrating solar power (CSP) plants with four different technologies by province in China: (A) Parabolic trough collector (PTC), (B) linear Fresnel collector (LFC), (C) central receiver system (CRS), and (D) parabolic dish system

(PDS).

3.3 CO_2 emission reduction potential

The life-cycle CO_2 emission intensity of CRS power generation is 0.035 $kgCO_2/kWh$, which is lower than existing power plants. Fig. 7 shows the potential for CO_2 emission reduction. If CSP plants had been constructed according to their technical potential under Scenario 1, the total amounts of CO_2 emission reductions in 2017, 2018 and 2019 would have reached 5.18×10^8, 5.61×10^8, and 6.24×10^8 t, respectively, accounting for 5.33%, 5.77%, and 6.41% of China's total CO_2 emissions in 2017, issued by China Emission Accounts and Datasets [70]. In terms of the distribution of CO_2 emission reduction potential by province, although Qinghai has high power generation potential, the CO_2 emission reduction potential is not high because of the low power demand of the province. In contrast, Inner Mongolia, Xinjiang, and other provinces with large power generation potential and large power demand have higher CO_2 emission reduction potential. Yunnan, Heilongjiang, and Hebei (limited by the CSP generation potential) are far from meeting their power demand, and their CO_2 emission reductions are limited. If power transmission between provinces could be fully realized under Scenario 2, the CO_2 emission reduction would reach 6.18×10^{10} t, which will exceed the global CO_2 emission of 5.6×10^{10} t predicted by the Intergovernmental Panel on Climate Change in a 2018 report [62]. In other words, if China was able to export CSP electricity to other countries, it could decarbonize the entire world.

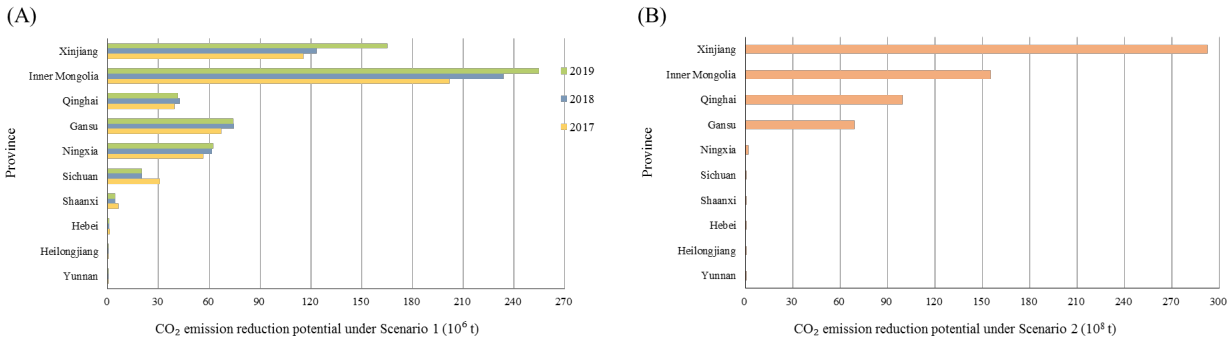

Fig. 7. CO_2 emission reduction potential of China's provinces: (A) Scenario 1, (B) Scenario 2.

3.4 Sensitivity analysis

The potential calculation in this study considers the surface slope and solar resources for geographic screening to clarify further the distribution of power generation potential under different geographic conditions and provide a reference for the actual construction of CSP plants. To explore sensitivities, the distribution of the power generation potential was calculated at different surface slopes and annual mean DNI values. The power generation potential when the annual mean DNI was higher than 1600 kWh/m^2 and the slope was less than 3° were taken as the zero reference point. The results of the sensitivity analysis are shown in Fig. 8. According to Fig. 8, when the minimum allowable annual DNI value is between 1000–1400 and 2400–2800 kWh/m^2, the total potential does not decrease significantly. The total potential is most sensitive to minimum annual DNI values between 1600 and 1800 kWh/m^2. When the DNI limit becomes more stringent at 1800 kWh/m^2, power generation decreases by approximately 30.19%. When the slope limit is relaxed to 5° or 7°, power generation increases by 10.72%–34.31% or 17.03%–57.24%, respectively. In the case of different land slopes, assuming that the mirror field with tracking device is arranged, the sunlight will be tracked according to the best angle. It means that the land slope only affects the suitable land area and then affects the power generation. In the case of DNI > 1600 kWh/m^2, when the slope limit becomes 5° and 7°, suitable areas increase to 1.13 × 10^6 and 1.19 × 10^6 km^2, respectively.

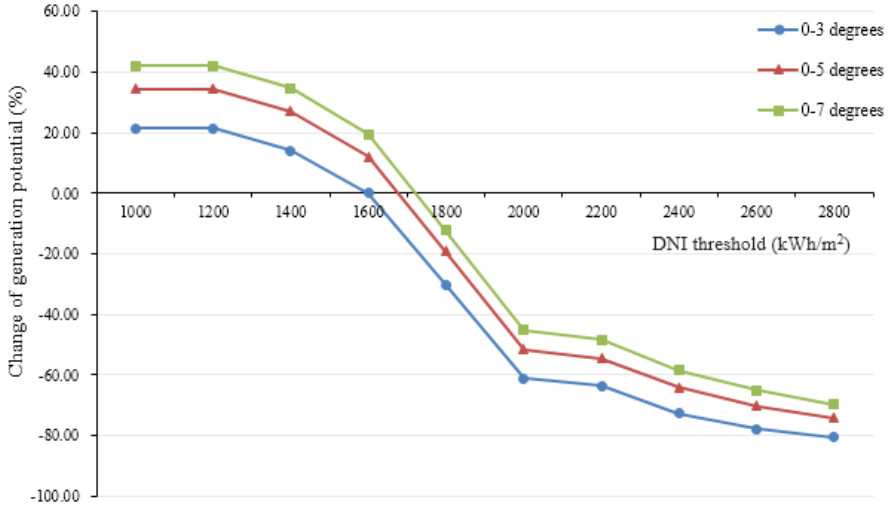

Fig. 8. Sensitivity analysis of generation potential based on different slope ranges and minimum direct normal irradiance (DNI).

3.5 Discussion

At present, little research has been conducted on evaluating China's CSP generation potential based on GIS; hence, it is difficult to compare the research results. The total power generation potential obtained in the present study is higher than He et al. [45]. This difference is mainly because the surface slope was set to a more stringent 1.7° in He et al., which leads to the omission of the power generation potential. Compared with similar studies, the innovation of the present study lies in the adoption of high-accuracy and high-precision solar irradiance and land-use data, accounting for water resource constraints and estimating the power generation potential of different types of CSP technologies by province. This provides a scientific basis and data base for industrial development and policy formulation.

Table 6 shows the CSP generation potential of China estimated in this research based on GIS and that of other countries or regions. It can be seen that CSP has great potential in China compared to these countries or regions because of large land areas and abundant solar radiation resources. Canada was poor in solar resources; only 1.30–4.18% of the area was suitable for the construction of CSP stations, according to the research by Djebbar et al [22]. Therefore, although China's total land area is smaller than that of Canada, its CSP generation potential is much larger than that of Canada. Sistan and Baluchistan province in Iran is not very rich in CSP resources [32]. About 12% of the areas are most suitable for CSP generation, with an average annual solar radiation of 1456 kWh/m^2 [32]. In the study of Ghasemi et al., the difference between specular area and specular field area was ignored, resulting in an overestimation of power generation potential [32]. Oman's land area is 1/31 of China's, but 82% of the land slope is less than 0.57° and is rich in solar resources [20]. The flat terrain is conducive to constructing a large-scale CSP station in Oman without additional cost to level the land. The land area of the United States is similar to that of China, and about 12% of the land is suitable for supporting the development of CSP [71]. This research proposes a complete research framework based on geographic constrains and technical constrains, and considers the impact of four CSP technologies and water resources differences in different provinces. Therefore, this framework can provide a theoretical

basis for similar research in other countries.

Table 6. Comparison of research on CSP generation potential in countries/regions based on GIS [20,22,32,71,72].

Country/region	Technical potential (10^{13} kWh/y)
Canada	0.83–2.62
Iran (Sistan and Baluchistan province)	0.74
Oman	0.76–1.37
Central Africa	2.99
Eastern Africa	17.58
Northern Africa	9.35
Southern Africa	14.96
Western Africa	2.27
United States	11.61
China (This research)	6.46–18.5

Owing to low power generation efficiency and high water consumption, the commercialization of CSP in China is relatively slow, and the current proportion in the grid is not large. Supercritical carbon dioxide (sCO_2) Brayton cycle power modules are among the most promising technologies to improve and replace current heat-to-electric conversion technologies [73]. It adopts sCO_2 as the working fluid, and the power generation cycle is a closed Brayton cycle [29]. Compared with the traditional steam turbine, the water demand of the whole system is significantly reduced, and the thermoelectric conversion efficiency is higher [29]. With the commercial operation of the sCO_2 Brayton cycle system in the future, it will gradually solve the problem that China's northwest region, rich in solar resources but lack water resources, is not suitable for the construction of large-scale CSP plants powered by steam turbines.

Ji et al. calculated the levelized cost of electricity (LCOE) of the CRS and PTC for 31 provinces in China, as shown in Table 7 [74]. Compared with other renewable energy

sources, the LCOE of the CSP station is relatively high [74]. The LCOE of the PTC with storage is relatively higher than that without storage, but lower than the CRS with storage [74]. Although the proportion of PTC in operating CSP plants globally is much larger than other technologies, CRS may be the leading technical direction of CSP in the future. From the perspective of provincial distribution, although Tibet has higher solar resources and lower LCOE than Xinjiang and Inner Mongolia, Tibet is not the most suitable province for constructing the CSP plants due to its relatively low suitable land areas. The LCOE of Sichuan and Yunnan is similar to that of Inner Mongolia, but they are still not suitable for developing CSP technology due to poor land suitability. Xinjiang has low LCOE and the largest proportion of the suitable land area. Therefore, Xinjiang is the most promising province in China to develop large-scale CSP technology.

Table 7. The LCOE of the CRS and PTC with 9-h storage of suitable provinces in China ($/MWh) [74]. LCOE - levelized cost of electricity.

Province	CRS with 9-h storage	PTC with 9-h storage
Tibet	142	186
Xinjiang	167	219
Qinghai	174	231
Gansu	203	266
Inner Mongolia	217	284
Sichuan	224	291
Yunnan	225	295
Ningxia	251	330
Heilongjiang	253	334
Shaanxi	255	342
Hebei	296	381

Combined with the research results and industry development status, the following

policy suggestions on the future development of CSP technology are put forward.

(1) In terms of power station project construction, the geographical and technical potential of CSP is concentrated in several provinces in Northwest China. Therefore, the focus should be on developing the northwest region with vast unused land areas. Under the same technical conditions, the land with abundant solar resources and the gentle slope is preferentially selected for project construction, to effectively utilize solar energy resources and obtain the best power generation performance.

(2) In terms of transmission side construction and electricity price management, the development of the CSP industry should be coordinated and promoted based on market demand and consumption. In the northwest region with rich resource potential, key trans-provincial power transmission channels such as transmission from the west to the east should be continued. This can also further promote China's carbon peaking and carbon neutrality goals, and maximize the carbon reduction potential of CSP technology. At the same time, the reform of the power system should be deepened to improve the market competitiveness of CSP power generation and further promote the reduction of LCOE.

(3) In terms of market scale, only 7 of the first batch of CSP demonstration projects were successfully connected to the grid. Therefore, the withdrawn and disqualified projects in the first batch of demonstration projects should be revitalized as soon as possible to expand market volume further. In addition, the complementary and coordinated development of CSP, photovoltaic, and wind power should be vigorously promoted. The core advantage of CSP is that it can complete the smooth output through the energy storage system. CSP, photovoltaic, and wind power can make full use of this advantage to achieve win-win results.

(4) In terms of technological development, LFC technology has greater technical potential than the other three technologies. However, since the technology has not yet reached commercial operation, the current market share is small. Therefore, investment in improving the CSP efficiency and reducing the costs should be increased, including improving the efficiency of the mirror field, reducing mirror costs, improving the efficiency of the heat transfer process, and reducing operating costs.

4. Conclusions

By collecting various geographic resource data and combining ArcGIS software, regions with the potential to develop CSP plants were screened considering geographic constraints. Then, based on technical constraints, the geographical, technical, and CO_2 emission reduction potential of CSP in China were evaluated by province.

The results show that China is rich in solar resources and has excellent CSP development potential. Approximately 11% of China's land is suitable for the construction of CSP stations, of which more than 99% is concentrated in five provinces in the northwest region (i.e., Xinjiang, Tibet, Inner Mongolia, Qinghai, and Ningxia). The current installed capacity of CSP of 420 MW is much lower than China's total potential installed capacity (2.45×10^7–5.40×10^7 MW) estimated in this study. The power generation potential is expected to be 6.46×10^{13}–1.85×10^{14} kWh, which is 8.91–25.52 times the national power consumption in 2019. The more extensive interval range is because of different CSP technologies. Future improvements in CSP conversion efficiencies will add to the power generation potential. Based on the assumption that if CSP plants replaced the existing power generators, the total CO_2 emission reduction potential of China in 2017, 2018, and 2019 would have reached 5.19×10^8, 5.61×10^8, and 6.24×10^8 t, respectively, which would have contributed to China's carbon reduction commitment. Assuming that the UHV power grid can fully satisfy the trans-regional power transmission, the CO_2 emission reduction of 6.18×10^{10} t can be achieved. Finally, combined with the development status of China's CSP industry and the research results, policy suggestions are put forward on China's CSP station project construction, transmission side construction and electricity price management, market scale, and technology development.

Acknowledgements

This research is supported by Open Fund of State Key Laboratory of Operation and Control of Renewable Energy & Storage Systems (China Electric Power Research Institute) (No.NYB51202101980).

References

[1] Energy & Climate Intelligence Unit. Net Zero Emissions Race, https://eciu.net/netzerotracker; 2021 [accessed 7 Sept 2021].

[2] Choi Y, Rayl J, Tammineedi C, Brownson JRS. PV Analyst: Coupling ArcGIS with TRNSYS to assess distributed photovoltaic potential in urban areas. Sol Energy 2011;85:2924–39. https://doi.org/10.1016/j.solener.2011.08.034.

[3] Kiefer CP, Caldés N, Río PD. Will dispatchability be a main driver to the European Union cooperation mechanisms for concentrated solar power? Energy Sources Part B 2021;16:42-54, https://doi.org/10.1080/15567249.2021.1885526.

[4] Bouhal T, Agrouaz Y, Kousksou T, Allouhi A, Rhafiki TE, Jamil A, et al. Technical feasibility of a sustainable Concentrated Solar Power in Morocco through an energy analysis. Renew Sustain Energy Rev 2018;81:1087–95. https://doi.org/10.1016/j.rser.2017.08.056.

[5] The 5th China Solar Thermal Power Conference. Assumption of large scale development of solar power generation, https://max.book118.com/html/2019/0904/6032010052002102.shtm; 2019. [accessed 7 June 2021].

[6] Casati E, Casella F, Colonna P. Design of CSP plants with optimally operated thermal storage. Sol Energy 2015;116:371–87. https://doi.org/10.1016/j.solener.2015.03.048.

[7] Pelay U, Luo L, Fan Y, Stitou D, Rood M. Thermal energy storage systems for concentrated solar power plants. Renew Sust Energ Rev 2017;79:82–100. https://doi.org/10.1016/j.rser.2017.03.139.

[8] Sha Y, Zhou M, Yang HJ, Liu SW, Li GY, Qi QR. Interconnected power system optimal operation with renewable generation considering flexibility of concentrating solar power plants & HVDC tie-line. Power System Technology 2020;44:3306–13.

[9] Chen GQ, Yang Q, Zhao YH, Wang ZF. Nonrenewable energy cost and greenhouse gas emissions of a 1.5 MW solar power tower plant in China. Renew Sust Energ Rev 2011;15:1961–7. https://doi.org/10.1016/j.rser.2010.12.014.

[10] Zhang Q, Cao D, Jiang K, Du X, Xu, E. Heat transport characteristics of a peak shaving solar power tower station. Renew Energ 2020;156:493–508. https://doi.org/10.1016/j.renene.2020.04.099.

[11] The Central People's Government of the People's Republic of China. Government Work Report, http://www.gov.cn/guowuyuan/zfgzbg.htm; 2021 [accessed 7 June 2021].

[12] Electric Power Development Research Institute. China Electrification Development Report (2019), https://www.cec.org.cn/upload/zt/2019report/; 2020 [accessed 7 June 2021].

[13] State Grid Corporation of China released the action plan of "carbon peaking and carbon neutralization", https://baijiahao.baidu.com/s?id=1693118969767306816&wfr=spider&for=pc; 2021 [accessed 7 June 2021].

[14] Sun YW, Hof A, Wang R, Liu J, Lin YJ, Yang DW. GIS-based approach for potential analysis of solar PV generation at the regional scale: A case study of Fujian Province. Energy Policy 2013;58:248–59. https://doi.org/10.1016/j.enpol.2013.03.002.

[15] CMA, Wind and Solar Energy Resources Center. China Wind and Solar Energy Resources Bulletin in 2019, https://news.bjx.com.cn/html/20200107/1034564.shtml; 2020 [accessed 7 June 2021].

[16] CMA Wind and Solar Energy Resources Center of China Meteorological Administration. Solar and Wind Energy Resource Inventory 2015, http://www.cma.gov.cn/2011xwzx/2011xqxxw/2011xqxyw/201602/t20160220_304586.html;2016 [accessed 7 June 2021].

[17] Ziuku S, Seyitini L, Mapurisa B, Chikodzi D, van Kuijk K. Potential of concentrated solar power (CSP) in Zimbabwe. Energy Sustain Dev 2014;23:220–7. https://doi.org/10.1016/j.esd.2014.07.006.

[18] Brewer J, Ames DP, Solan D, Lee R, Carlisle J. Using GIS analytics and social preference data to evaluate utility-scale solar power site suitability. Renew Energy 2015;81:825–36. https://doi.org/10.1016/j.renene.2015.04.017.

[19] Anwarzai MA, Nagasaka K. Utility-scale implementable potential of wind and solar energies for Afghanistan using GIS multi-criteria decision analysis. Renew Sust Energ Rev 2017;71:150–60. https://doi.org/10.1016/j.rser.2016.12.048.

[20] Gastli A, Charabi Y. Solar electricity prospects in Oman using GIS-based solar radiation maps. Renew Sustain Energy Rev 2010;14:790–7. https://doi.org/10.1016/j.rser.2009.08.018.

[21] Uyan M. GIS-based solar farms site selection using analytic hierarchy process (AHP) in Karapinar region, Konya/Turkey. Renew Sustain Energy Rev 2013;28:11–7.

https://doi.org/10.1016/j.rser.2013.07.042.

[22] Djebbar R, Belanger D, Boutin D, Weterings E, Poirier M. Potential of concentrating solar power in Canada. Energy Procedia 2014;49:2303–12. https://doi.org/10.1016/j.egypro.2014.03.244.

[23] Janke JR. Multicriteria GIS modeling of wind and solar farms in Colorado. Renew Energy 2010;35:2228–34. https://doi.org/10.1016/j.renene.2010.03.014.

[24] Hermann S, Miketa A, Fichaux N. Estimating the renewable energy potential in Africa: A GIS-based approach; IRENA Working Paper; International Renewable Energy Agency: Abu Dhabi, UAE, 2014.

[25] Giamalaki M, Tsoutsos T. Sustainable siting of solar power installations in Mediterranean using a GIS/AHP approach. Renew Energ 2019;141:64–75. https://doi.org/10.1016/j.renene.2019.03.100.

[26] Sharma C, Sharma AK, Mullick SC, Kandpal TC. Assessment of solar thermal power generation potential in India. Renew Sust Energ Rev 2015;42:902–12. https://doi.org/10.1016/j.rser.2014.10.059.

[27] Dawson L, Schlyter P. Less is more: Strategic scale site suitability for concentrated solar thermal power in Western Australia. Energy Policy 2012;47:91-101. https://doi.org/10.1016/j.enpol.2012.04.025.

[28] Damerau K, Williges K, Patt AG, Gauché P. Costs of reducing water use of concentrating solar power to sustainable levels: Scenarios for North Africa. Energy Policy 2011;39:4391–8. https://doi.org/10.1016/j.enpol.2011.04.059.

[29] Yuan XX, Zhang XB. Demonstration of Supercritical Carbon Dioxide BraytonCycle in Solar Thermal Power Generation. Dongfang Turbine 2021;01:33–8.

[30] Tlhalerwa K, Mulalu M. Assessment of the concentrated solar power potential in Botswana. Renew Sust Energ Rev 2019;109:294–306. https://doi.org/10.1016/j.rser.2019.04.019.

[31] Aly A, Jensen SS, Pedersen AB. Solar power potential of Tanzania: Identifying CSP and PV hot spots through a GIS multicriteria decision making analysis. Renew Energ 2017;113:159–75. https://doi.org/10.1016/j.renene.2017.05.077.

[32] Ghasemi G, Noorollahi Y, Alavi H, Marzband M, Shahbazi M. Theoretical and technical potential evaluation of solar power generation in Iran. Renew Energ 2019;138:1250–61. https://doi.org/10.1016/j.renene.2019.02.068.

[33] Merrouni AA, Mezrhab A, Mezrhab A. CSP sites suitability analysis in the Eastern region of

Morocco. Energy Procedia 2014;49: 2270–9. https://doi.org/10.1016/j.egypro.2014.03.240.

[34] Yushchenko A, De Bono A, Chatenoux B, Patel MK, Ray N. GIS-based assessment of photovoltaic (PV) and concentrated solar power (CSP) generation potential in West Africa. Renew Sust Energ Rev 2017;81:2088–103.

[35] Boukelia TE, Mecibah MS. Parabolic trough solar thermal power plant: Potential, and projects development in Algeria. Renew Sust Energ Rev 2013;21:288–97. https://doi.org/10.1016/j.rser.2012.11.074.

[36] Talebizadeh P, Mehrabian MA, Abdolzadeh M. Prediction of the optimum slope and surface azimuth angles using the Genetic Algorithm. Energy Build 2011;43:2998-3005. https://doi.org/10.1016/j.enbuild.2011.07.013.

[37] Keshavarz SA, Talebizadeh P, Adalati S, Mehrabian MA, Abdolzadeh M. Optimal Slope-Angles to Determine Maximum Solar Energy Gain for Solar Collectors Used in Iran. Int. J. Renew. Energy Res 2012;2:665-73.

[38] Talebizadeh P, Mehrabian MA, Rahimzadeh H. Optimization of Heliostat Layout in Central Receiver Solar Power Plants. J. Energy Eng 2014;140:04014005. https://doi.org/10.1061/(ASCE)EY.1943-7897.0000162.

[39] Purohit I, Purohit P. Technical and economic potential of concentrating solar thermal power generation in India. Renew Sust Energ Rev 2017;78:648–667. https://doi.org/10.1016/j.rser.2017.04.059.

[40] Charabi Y, Gastli A. GIS assessment of large CSP plant in Duqum, Oman. Renew Sust Energ Rev 2010;14:835–41. https://doi.org/10.1016/j.rser.2009.08.019.

[41] Wang JF, Meng B, Li LF. A location choice model of solar heat power plant in China. Journal of Geo-Information Science 2007;9:43–8.

[42] Zhao MZ, Song SJ, Zhang XM. A selection method of trough solar thermal power station siting at a micro level. Renew Energ Resour 2013;3:18–22.

[43] Zhao MZ, Jiang X, Song SJ. Development situation and potential analysis about Parabdic Trough solar thermal power technique in China. Energ Engineer 2013;2:27–30.

[44] Wu Y, Zhang B, Wu C, Zhang T, Liu F. Optimal site selection for parabolic trough concentrating solar power plant using extended PROMETHEE method: A case in China. Renew Energ 2019;143:1910–27. https://doi.org/10.1016/j.renene.2019.05.131.

[45] He G, Kammen DM. Where, when and how much solar is available? A provincial-scale solar resource assessment for China. Renew Energ 2016;85:74–82. https://doi.org/10.1016/j.renene.2015.06.027.

[46] NEA. Notice of the National energy Administration on the Construction of Solar Thermal Power Generation Demonstration Projects. http://zfxxgk.nea.gov.cn/auto87/201609/t20160914_2298.htm; 2016[accessed 7 June 2021].

[47] Ling-Zhi R, Xin-Gang Z, Xin-Xuan Y, Yu-Zhuo Z. Cost-benefit evolution for concentrated solar power in China. J Clean Prod 2018;190:471–82. https://doi.org/10.1016/j.jclepro.2018.04.059.

[48] Clifton J, Boruff BJ. Assessing the potential for concentrated solar power development in rural Australia. Energy Policy 2010;38:5272–80. https://doi.org/10.1016/j.enpol.2010.05.036.

[49] Liu J, Xu F, Lin S. Site selection of photovoltaic power plants in a value chain based on grey cumulative prospect theory for sustainability: A case study in Northwest China. J Clean Prod 2017;148:386–97. https://doi.org/10.1016/j.jclepro.2017.02.012.

[50] NEA. Notice on Organizing the Construction of Solar Thermal Power Demonstration Projects. http://zfxxgk.nea.gov.cn/auto87/201509/t20150930_1968.htm; 2015[accessed 7 June 2021].

[51] Ministry of Housing and Urban-Rural Development of the People's Republic of China. Design standard for tower solar thermal power station. http://www.mohurd.gov.cn/wjfb/201904/t20190402_240025.html; 2018 [accessed 7 June 2021].

[52] Turney D, Fthenakis V. Environmental impacts from the installation and operation of large-scale solar power plants. Renew Sust Energ Rev 2011;15:3261–70. https://doi.org/10.1016/j.rser.2011.04.023.

[53] Sun R. Promote the healthy development of solar thermal power generation and help the steady implementation of energy transformation. China Energy News 2020;025.

[54] IRENA. Unleashing the solar potential in ECOWAS: Seeking areas of opportunity for grid-connected and decentralised PV applications. An opportunity-based approach. International Renewable Energy Agency 2013.

[55] Concentrating solar power commercial application study: Reducing water consumption of concentrating solar power electricity generation. U.S. Department of Energy. 2010;1–35.

[56] Aseri TK, Sharma C, Kandpal TC. Assessment of water availability for wet cooling at potential locations for solar thermal power generation in India. Int J Ambient Energy 2018;41:1126–41.

https://doi.org/10.1080/01430750.2018.1507926.

[57] Wang ZF. Design of solar thermal power plants. Beijing: Chemical Industry Press 2012;10:241.

[58] Duvenhage DF, Brent AC, Stafford WHL, Van Den Heever D. Optimising the concentrating solar power potential in South Africa through an Improved GIS Analysis. Energies 2020;13:3258. https://doi.org/10.3390/en13123258.

[59] Ong S, Campbell C, Denholm P, Margolis R, Heath G. Land-use Requirements for solar power plants in the United States. National Renewable Energy Laboratory, https://www.nrel.gov/docs/fy13osti/56290.pdf; 2013 [accessed 7 June 2021].

[60] Viebahn P, Lechon Y, Trieb F. The potential role of concentrated solar power (CSP) in Africa and Europe—a dynamic assessment of technology development, cost development and life cycle inventories until 2050. Energy Policy 2011;39:4420–30. https://doi.org/10.1016/j.enpol.2010.09.026.

[61] National Renewable Energy Laboratory. Concentrating Solar Power Projects. https://solarpaces.nrel.gov/; [accessed 7 June 2021].

[62] Yang Q, Huang TY, Wang SG, Li JS, Dai SQ, Wright S, et al. A GIS-based high spatial resolution assessment of large-scale PV generation potential in China. Appl Energ 2019;247:254–69. https://doi.org/10.1016/j.apenergy.2019.04.005.

[63] National Bureau of Statistics of China. China statistical yearbook. [Chinese version] http://www.stats.gov.cn/tjsj/ndsj/2020/html/C0914.jpg; 2020 [accessed 7 June 2021].

[64] Institute for Global Environmental Strategies. IGES list of grid emission factors (version 10.9). https://www.iges.or.jp/en/pub/list-grid-emission-factor/en; 2020 [accessed 7 June 2021].

[65] Marnay C, Fisher D, Murtishaw S, Phadke A, Price L, Sathaye J. Estimating carbon dioxide emissions factors for the California electric power sector. Berkeley: Lawrence Berkeley National Laboratory; 2002.

[66] Li RX, Zhang HR, Wang HR, Tu QS, Wang XJ. Integrated hybrid life cycle assessment and contribution analysis for CO_2 emission and energy consumption of a concentrated solar power plant in China. Energy 2019;174:310–22.

[67] Ren LZ, Zhao XG , Yu XX, Zhang YZ. Cost-benefit evolution for concentrated solar power in China. J Clean Prod 2018;190:471–82. https://doi.org/10.1016/j.jclepro.2018.04.059.

[68] Islam MT, Huda N, Abdullah AB, Saidur R. A comprehensive review of state-of-the-art

concentrating solar power (CSP) technologies: Current status and research trends. Renew Sustain Energy Rev 2018;91:987–1018. https://doi.org/10.1016/j.rser.2018.04.097.

[69] SolarPACES. CSP projects around the world. SolarPACES. https://www.solarpaces.org/csp-technologies/csp-projects-around-the-world/;2018 [accessed 7 June 2021].

[70] China Emission Accounts and Datasets. National Emission Inventory 2016–2017. https://www.ceads.net.cn/[accessed 7 January 2021].

[71] Lopez A, Roberts B, Heimiller D, Blair N, Porro G. U.S.Renewable Energy Technical Potentials: A GIS-Based Analysis. National Renewable Energy Laboratory (NREL) 2012. https://www.nrel.gov/docs/fy12osti/51946.pdf [accessed on 11 October 2021].

[72] Hermann S, Miketa A, Ficaux N. Estimating the renewable energy potential in Africa: A GIS-based approach. International Renewable Energy Agency (IRENA) 2014. https://www.irena.org/-/media/Files/IRENA/Agency/Publication/2014/IRENA_Africa_Resource_Potential_Aug2014.pdf [accessed on 11 October 2021].

[73] Sorbet FJ, Mendoza M, J García-Barberena. Performance evaluation of CSP power tower plants schemes using supercritical carbon dioxide Brayton power block. International Conference on Concentrating Solar Power and Chemical Energy Systems 2019. https://doi.org/10.1063/1.5117568.

[74] Ji JP, Tang H, Jin P. Economic potential to develop concentrating solar power in China: A provincial assessment. Renewable and Sustainable Energy Reviews 2019;114:109279. https://doi.org/10.1016/j.rser.2019.109279.